Triggered Release of Pharmacophores from [Ni(HAsO$_3$)]-Loaded Polymer-Caged Nanobin Enhances Pro-apoptotic Activity: A Combined Experimental and Theoretical Study

Sang-Min Lee,[†] One-Sun Lee,[†] Thomas V. O'Halloran,[*] George C. Schatz,[*] and SonBinh T. Nguyen[*]

Department of Chemistry and Center of Cancer Nanotechnology Excellence, Northwestern University, 2145 Sheridan Road, Evanston, Illinois 60208-3113, United States. [†] These authors contributed equally to this work.

ABSTRACT Nanoscale drug delivery platforms can provide an attractive therapeutic strategy for cancer treatments, as they can substantially reduce the adverse side effects associated with toxic small-molecule anticancer agents. For enhanced therapeutic efficacy to be achieved with such platforms, a tumor-specific drug-release trigger is a critical requirement. This article reports the use of a pH-sensitive polymer network that surrounds a nanoscale liposome core to trigger the release of both encapsulated hydrophilic, membrane-impermeable Ni^{II} cations and amphipathic, membrane-permeable As^{III} anticancer agents under acidic conditions commonly encountered in hypoxic tumor tissues and late endosomes. Computational modeling studies provide clear evidence that the acid-triggered drug-release mechanism for this polymer-caged nanobin (PCN) platform arises from a pH- and temperature-responsive conformation change of the cross-linked polymer cage. As a result, the simultaneous release of both of the active agents in this multicomponent therapeutic enhances the pro-apoptotic activity of As^{III} while diminishing its acute toxicity, potentially reducing the undesirable side effects commonly associated with this free drug. The ability to engender acid-triggered release of drugs co-encapsulated inside a liposomal template makes drug delivery using PCN an attractive strategy for triggered drug release.

KEYWORDS: polymer · liposome · drug delivery · pH-sensitive release · molecular modeling · arsenic trioxide

Drug delivery using nanoscale liposomal vehicles has recently emerged as a highly promising strategy for cancer treatments with many advantages over conventional small-molecule chemotherapy.[1] Such advantages, arising from the ability of liposomes to encapsulate cytotoxic drugs and protect them from enzymatic degradation and renal clearance, include improved pharmacokinetics and reduced adverse side effects often associated with toxic small-molecule anticancer agents.[2] Together with the use of ion gradient-mediated (IGM) loading methodology, liposomal cores can be infused with very high density of drugs (0.3−0.5 drug-to-lipid molar ratio, often beyond the aqueous solubility of these drugs).[3,4] These features allow for the delivery of a high dosage of pharmaceuticals while maintaining low side effects and are responsible in part for the clinical successes of a number of liposomal formulations in the treatment of cancer.[1,5]

Recently, an IGM-based method has been developed to load arsenic trioxide (ATO, As_2O_3) into liposomes as nanoparticulate aggregates of hydrated arsenite anions ($[M(HAs^{III}O_3)]_n$) in the presence of several transition metal ions,[6] including Co^{II}, Ni^{II}, and Zn^{II}, or aquated cisplatin complex.[7] Arsenic trioxide (Trisenox, Cephalon Inc., Frazer, PA) is an emerging anticancer drug possessing pro-apoptotic and antiangiogenic activity,[8,9] whose therapeutic effectiveness has been demonstrated against acute promyelocytic leukemia[10] and several solid tumors.[11,12] Additionally, Ni^{II} has been shown to potentiate the anticancer activity of As^{III},[6,13] *via* a mechanism that involves the depletion of glutathione and ascorbate,[14] both of which are known to play an important role in modulating the toxicity of intracellular heavy metal ions to protect the cells from apoptosis. Interestingly, while [Ni^{II}, As^{III}]-encapsulated liposomes have demonstrated excellent *in vivo* tumor-growth suppression,[12] better than free ATO, the Ni^{II} and As^{III} ions are not released in a concerted manner *in vitro*. In solution-based release assays,[6,12] only As^{III} was released readily as membrane-permeable arsenous acid, while the Ni^{II} ions are still trapped inside the intact liposomal vehicles after 48 h of incubation under acidic conditions.

We previously demonstrated the insertion/cross-linking of cholesterol-terminated poly(acrylic acid) as a facile *drop-in* modification

* Address correspondence to t-ohalloran@northwestern.edu (for liposome synthesis, inorganic synthesis, and biology); schatz@chem.northwestern.edu (for molecular modeling); and stn@northwestern.edu (for polymer and PCN synthesis, characterization, and study).

Received for review February 5, 2011 and accepted April 5, 2011.

Published online April 05, 2011
10.1021/nn200478m

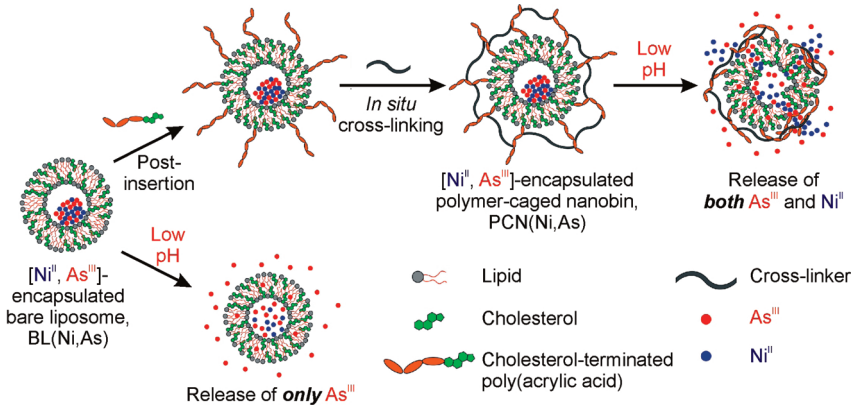

Scheme 1. Schematic representation of PCN synthesis and how the polymer cage can be used to control the release of encapsulated drug molecules.

strategy for stabilizing drug-loaded liposomes without hampering the encapsulated drug.[15] The resulting polymer-caged nanobins (PCN) possess pH-sensitive polymer shells that can enhance the release of the encapsulated drugs in acidic environments commonly found in tumor interstitium[16] and cellular endosomes.[17] As such, we hypothesize that the PCN platform can be used to modulate the therapeutic efficacy of the [Ni^{II}, As^{III}]-encapsulated liposome system *via* acid-triggered release of both As^{III} and Ni^{II} ions at the same time.

Herein, we demonstrate the versatility of the pH-sensitive polymer cage of the PCN platform in inducing release of both pharmacologically active types of cargo (namely As^{III} and Ni^{II}) that have been co-encapsulated in a single liposomal core (Scheme 1), which leads to better pro-apoptotic activity in cancer cell lines. Molecular modeling further confirms that this chemomechanical release property of the PCN arises from stimuli-responsive conformational change of the polymer cage, which in turn perturbs the lipid membrane. Thus, triggered drug release in PCNs that in a quite different manner than that in the bare liposomes, BL(Ni,As), which have no PEG or other polymer coating. The resulting concurrent release of As^{III} and Ni^{II} ions from a single PCN can cooperatively enhance the pro-apoptotic activity of the combined drugs while showing lower acute toxicity than either free ATO or [Ni^{II}, As^{III}]-encapsulated BL.

RESULTS AND DISCUSSION

Synthesis and Characterization of [Ni^{II}, As^{III}]-Encapsulated Polymer-Caged Nanobin, PCN(Ni,As). [Ni^{II}, As^{III}]-encapsulated bare liposomes, BL(Ni,As), were first prepared from aqueous ATO and nickel acetate (Ni(CH$_3$COO)$_2$) using a previously reported IGM drug-loading protocol.[6] During the IGM loading of As^{III}, neutral arsenous acid (H_3AsO_3, a water-soluble As^{III} species with high membrane-permeability)[18] molecules can remotely diffuse across the liposomal membrane to form an insoluble nickel arsenite complex, $[Ni(HAsO_3)]_n$, inside the liposomal core (Scheme S1 in the Supporting Information (SI)).[6] Using the resulting BL (Ni,As) (arsenic-to-lipid ratio = 0.45 ± 0.03 mol/mol as determined by inductively coupled plasma optical emission spectroscopy, ICP-OES; D_H (hydrodynamic diameter) = 98 ± 7 nm and ζ (zeta potential) = −4.1 mV as measured by dynamic light scattering (DLS) at 25 °C) as a template, PCN(Ni,As) was subsequently constructed *via* the insertion of cholesterol-terminated poly(acrylic acid) (Chol-PAA, $\bar{M}_n \approx 3700$ Da) into the membrane, followed by *in situ* cross-linking with 2,2′-(ethylenedioxy)-bis(ethylamine)[19] (Figure 1). The hydrodynamic diameter of the resulting PCN(Ni,As) increases to 121 ± 17 nm (ζ = −14.2 mV), while its arsenic-to-lipid ratio remains essentially unchanged (0.44 ± 0.04 mol/mol). As expected from our previous stability study of a similar dye-loaded system,[20] PCN(Ni,As) is also quite stable under biological pH and temperature, maintaining a constant hydrodynamic diameter over five days (Figure S1 in the SI).

Acid-Triggered Release of Ni^{II} and As^{III} from PCN(Ni,As). As our previously reported doxorubicin-encapsulated PCN has exhibited increased drug-release property under acidic conditions,[15] similar enhancement of cargo release was expected with [Ni^{II}, As^{III}]-encapsulated PCNs. Indeed, when PCN(Ni,As) and BL(Ni,As) were incubated at pH 4.0 and 37 °C, their As^{III}-release rates were both enhanced. Surprisingly, a significant enhancement in Ni^{II}-release by PCN(Ni,As) (apparent release rate $k_{PCN}(Ni^{II}) = 8.25\ h^{-1}$) over BL(Ni,As) ($k_{BL}(Ni^{II}) < 1.0\ h^{-1}$, Table 1) was observed. More than 50% of the Ni^{II} payload was released from PCN(Ni,As) after 12 h, while a negligible amount of Ni^{II} was released from BL(Ni,As) during this same time period (Figure 2). As hypothesized previously,[20] this enhanced release can be attributed to the protonation of the free acrylate groups in the cross-linked polymer cage at low pH, which increases the local density of the cage on the PCN(Ni,As) surface (see discussion in the modeling sections below), ultimately leading to the collapse of the liposomal membrane and the release of aqueous Ni^{II} ions. Such a release mechanism does not exist in BL(Ni,As), where the aqueous Ni^{II} ions remain unreleased

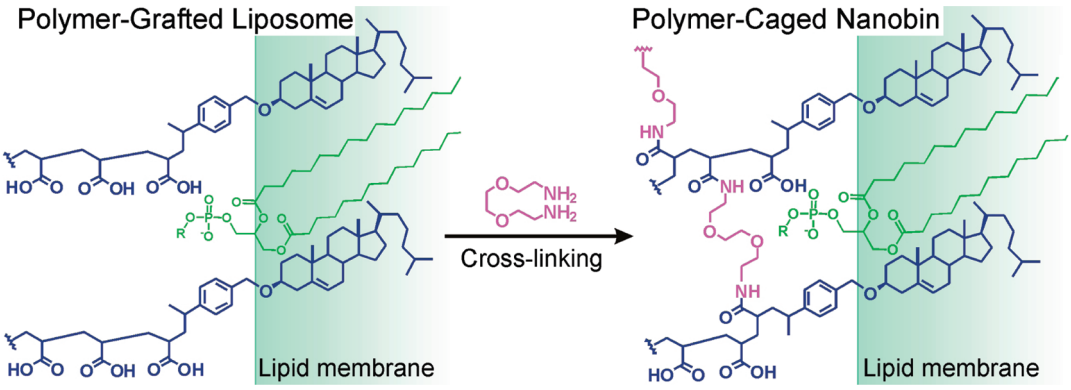

Figure 1. Chemical structures of the cross-linked polymer network in polymer-grafted liposome (left) and polymer-caged nanobins (PCN, right).

TABLE 1. pH-Dependence of the Apparent Cargo-Release Rates

pH	sample	$k^{apr}_{release}$ (Ni^{II})	$k^{apr}_{release}$ (As^{III})
7.4	PCN(Ni,As)	<1.0	1.4
7.4	BL(Ni,As)	<1.0	1.5
4.0	PCN(Ni,As)	8.25	14.7
4.0	BL(Ni,As)	<1.0	27.9

inside the liposomal core after the arsenous acid component diffuses out of the membrane.[6,12]

Interestingly, the apparent release rate of As^{III} from PCN(Ni,As) was only about half of that from BL(Ni,As). We ascribed this to increased H-bonding interactions between the amphipathic arsenous acid ($As(OH)_3$), the fully protonated form of aqueous As^{III} under acidic conditions, and the collapsed hydrophobic polymer–lipid shell. This interaction is likely inhibiting the free diffusion of As^{III} species into the surrounding media.[21] Together with the aforementioned increased release of Ni^{II}, this result suggests that the release profiles of both aqueous Ni^{II} and amphipathic As^{III} can indeed be modulated by the pH-tunable hydrophobic nature of the polymer cage surrounding the PCN(Ni,As).

Enhanced *in Vitro* Apoptosis Activity of the [Ni^{II}, As^{III}] Drug Combination in PCN(Ni,As). Because Ni^{II} ions, which are known to deplete cellular antioxidants such as glutathione and ascorbate,[14] can be released in an enhanced manner from PCN(Ni,As), we evaluated its combined effect with As^{III} in the PCN(Ni,As) formulation against HeLa human cervical cancer cells. HeLa cells were exposed to 10 μM [As^{III}] solutions of PCN(Ni,As), BL(Ni,As), and free ATO for 48 h at 37 °C before the apoptotic/dead cell populations were measured by annexin-V/7-AAD assay.[22] We observe a 1.7-fold higher apoptotic cell population ($\sim$12.1 $\pm$ 2.3%, Figure 3A) for HeLa cells treated with PCN(Ni,As) compared to those treated with BL(Ni,As) ($\sim$7.0 $\pm$ 1.6% apoptotic population, Figure 3A). As higher apoptotic cell populations can be correlated to higher susceptibilities of cancer cells toward a chemotherapeutic platform, this result

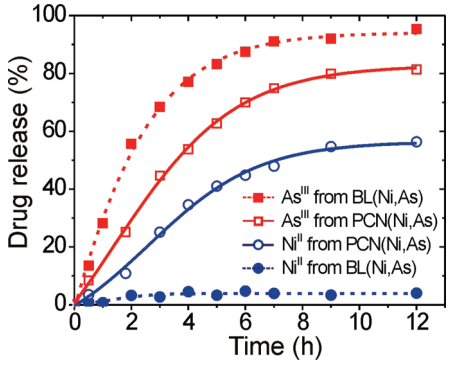

Figure 2. Release profiles of Ni^{II} and As^{III} ions from bare liposome, BL(Ni,As), and polymer-caged nanobins, PCN(Ni,As), at pH 4.0 and 37 °C.

suggests that PCN(Ni,As) should have enhanced therapeutic activity against tumors compared to BL(Ni,As).

The aforementioned results suggest that while less As^{III} may be released from PCN(Ni,As) than from BL(Ni,As) under endosomal conditions, the concurrent release of Ni^{II} from PCN(Ni,As) can cooperatively increase the pro-apoptotic activity of As^{III} drugs, leading to a higher ratio of apoptotic-to-dead cells, and thus better efficacy, with PCN(Ni,As). This cooperativity is striking when one considers that both liposomal Ni^{II} and free Ni^{II} ions have been reported to have negligible cytotoxicity against HeLa cells at concentrations less than 30 μM,[13] in the range where our apoptosis assays with PCN(Ni,As) were performed (10–12 μM of Ni^{II} ions). In fact, treating HeLa cells with free Ni^{II} ions resulted in no cytotoxicity up to 80 μM,[13] presumably because the hydrophilic Ni^{II} ions cannot pass through the cell membranes. These observations suggest that the encapsulation of both Ni^{II} and As^{III} in PCN(Ni,As) can lead to enhanced therapeutic behavior from a combination of enhanced endocytotic uptake[23] and concurrent release. PCN(Ni,As) may have an additional therapeutic benefit relative to BL(Ni,As) if the enhanced pro-apoptotic capability can be translated into *in vivo* reduced acute toxicity that causes detrimental side effects to patients.

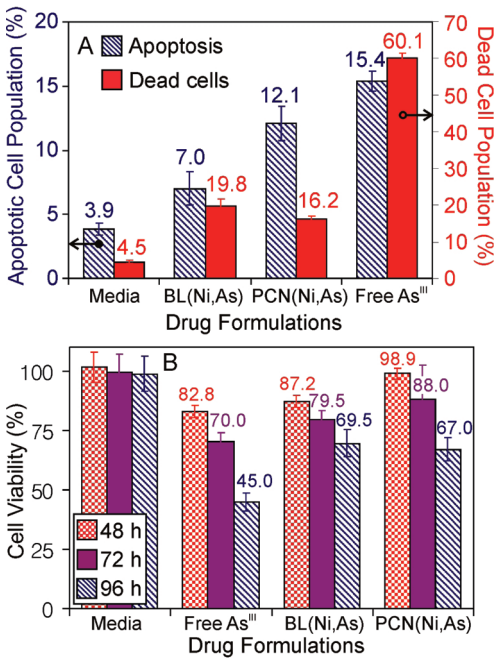

Figure 3. (A) Apoptotic effect of As^{III}-containing drug formulations. HeLa human cervical cells were treated with solutions of PCN(Ni,As), BL(Ni,As), and free ATO ($[As^{III}] = 10\ \mu M$ for each formulation) for 48 h before being analyzed by annexin-V/7-AAD assay.[22] The average percent populations of apoptotic and dead cells are indicated directly on top of each bar. (B) Relative viability of HeLa cells in the presence of As^{III}-containing formulations. Cells were incubated with solutions of PCN(Ni,As), BL(Ni,As), and free ATO ($[As^{III}] = 10\ \mu M$ for each formulation) for 48, 72, and 96 h before being analyzed by MTS cell proliferation assay.[24] Aqueous ATO (As_2O_3) was used as a control (free As^{III}) in both experiments because metal arsenite complexes such as $[Ni(HAsO_3)]$ have very low solubility and cannot be dissolved in aqueous solution.[18] We note that the two assays cannot be directly compared; the annexin-V/7-AAD assay measured the proportions of apoptotic and dead cells in a culture, while the % cell viability in the MTS assay has to be measured against an external culture grown in the media as a control.

While PCN(Ni,As) is less cytotoxic than BL(Ni,As) at short incubation times, its cytotoxicity against HeLa cells approaches that of BL(Ni,As) as the cellular drug-exposure time increases (Figure S4 in the SI). At 10 μM $[As^{III}]$, cells exposed to PCN(Ni,As) retain 99% cell viability after a 48 h incubation, less toxic than BL(Ni, As) (87% cell viability) and free ATO (83% cell viability, Figure 3B). After 96 h of incubation, however, the cytotoxicity of PCN(Ni,As) (67% cell viability) is the same as that for BL(Ni,As) (69% cell viability). This phenomenon may be explained in part by the 2-fold slower release of As^{III} from PCN(Ni,As) under acidic conditions compared to that from BL(Ni,As) (Table 1). Assuming that both types of particles are taken up *via* endocytosis,[23,25] the acidic environment of the endosome will result in a slower release of As^{III} pharmacophore from PCN(Ni,As), which in turn leads to a lower cytotoxicity at shorter exposures. We suggest that the higher release rate of Ni^{II} from PCN(Ni,As) (Table 1) began to reduce the intracellular glutathione concentration during this period and gradually enhanced the ability of the small amount of As^{III} agents available to induce apoptosis (Figure 3A).[26]

TABLE 2. Half-Maximal Inhibitory Concentration (IC_{50}, values are in μM)

drug formulation	IC_{50} at 48 h (μM)	IC_{50} at 72 h (μM)	IC_{50} at 96 h (μM)
free ATO	26.2 ± 3.4	20.2 ± 3.5	10.7 ± 2.8
BL(Ni,As)	39.3 ± 4.1	27.5 ± 4.4	22.6 ± 3.7
PCN(Ni,As)	103.4 ± 9.7	55.2 ± 7.7	30.2 ± 5.3

The IC_{50} values of PCN(Ni,As), BL(Ni,As), and free ATO against HeLa cells at different exposure times are listed in Table 2, showing a progressively narrowing gap between the values for PCN(Ni,As) and those for BL(Ni,As) and free ATO as incubation time increases. This is not surprising given previous reports[12,27] that nanoencapsulated drugs generally exhibit much attenuated initial *in vitro* toxicity compared to the free drugs due to the slower drug release kinetics from the carrier particles. The slow release of drugs from nanoencapsulated carriers in general has been suggested as one reason for the reduction of the acute toxicity of the parent drugs *in vivo*,[2,5] allowing for higher dosing with fewer detrimental side effects and thus better patient cure and survival. Indeed, several related packaged formulations exhibit lower *in vitro* toxicity compared to the free drugs and show excellent enhancements in *in vivo* therapeutic efficacies,[12,28,29] presumably *via* the well-known "enhanced permeation and retention (EPR)" effect.[30] Coupled to this reduction in acute toxicity, the improved combination of drug-release property and the enhanced pro-apoptotic capability of PCN(Ni,As) suggests that this platform should have excellent potential for *in vivo* therapeutic activity.

Understanding the pH-Dependent Release Property of the PCN(Ni,As) System *via* Computer Modeling of the Polymer Configuration. We previously attributed the acid-triggered drug-release property of the PCN platform to the pH-sensitive aggregation of the cross-linked polymer cage,[20] which is comprised of randomly distributed acrylic acid (AAc) and acrylamide (AAm) groups. This hypothesis was inspired by the known acidity-induced random-coil-to-globule phase transition of the random copolymer of acrylic acid and acrylamide, poly(AAc-*r*-AAm), in aqueous solution,[31] where the pH-dependent ionization of the acrylic acid groups was shown to play a critical role in volume shrinkage of the polymer network,[32] following Flory–Huggins theory.[33,34] To further test this hypothesis, we carried out Monte Carlo (MC) simulations to compare the global minimum structures of amide-modified poly(acrylate), a molecular analogue of our polymer cage (Figure S5 in the SI), at two different pHs.

A molecular model of a random copolymer composed of AAc and AAm groups (20-mers of each group, totaling 40 repeating units) was used to simulate the

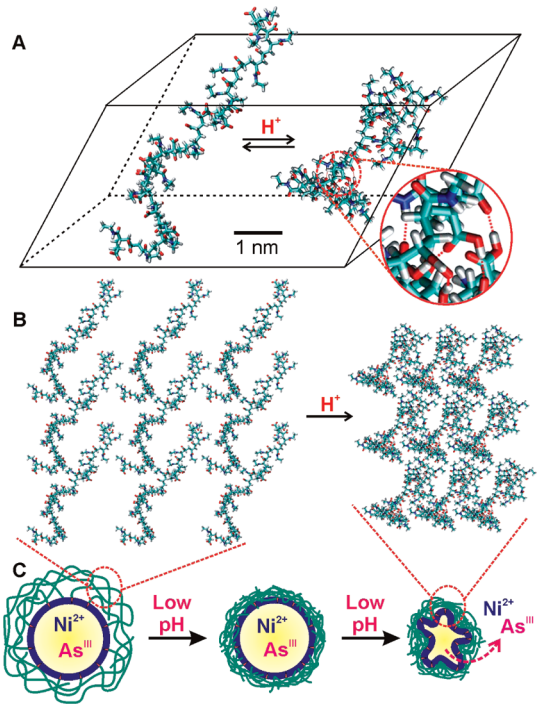

Figure 4. (A) Globally minimized structures of a model poly(AAc-*r*-AAm) polymer with different protonation states obtained from Monte Carlo (MC) simulations. The radius of gyration (R_G) for the deprotonated polymer at neutral pH (left) is 19.1 Å, and that for the protonated polymer under aqueous acidic conditions (right) is 11.6 Å. The zoom-in view of a section of the collapsed polymer (right) clearly shows the formation of intrachain hydrogen bonds, as indicated by red lines. (B) Stacked plot of several polymer "unit cells" showing the increase in density when a conglomeration of polymer chains under neutral (left) conditions is subjected to an acidic (right) environment. (C) Schematic representation of the macroscopic consequence of the acid-triggered densification, and subsequent collapse, of the cross-linked polymer cage on a PCN(Ni,As) leading to enhanced release of Ni^{II} and As^{III} ions.

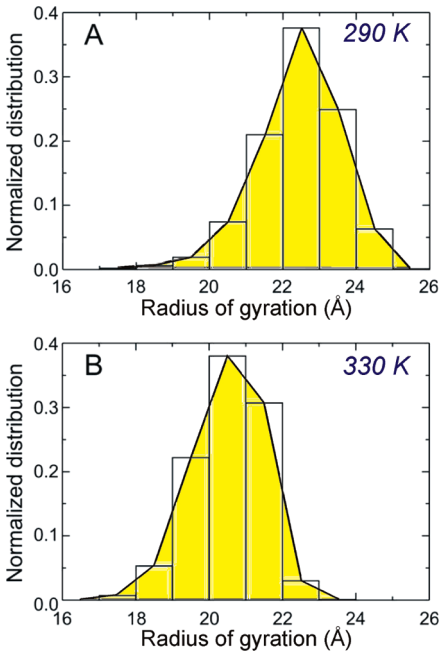

Figure 5. Normalized distributions of the radius of gyration (R_G) of poly(AAc-*r*-AAm) estimated from molecular dynamics simulations for 1 ns at (A) 290 K (average $R_G = 22.4 \pm 1.1$ Å) and (B) 330 K (average $R_G = 20.5 \pm 0.9$ Å).

50% cross-linked polymer cage in PCN(Ni,As). The global minimum conformations of this polymer chain at virtual pH 7.4 and 5.0 were determined using a MC conformation search method[35] in water, showing dramatic pH-dependent conformational changes. Under neutral conditions, the model polymer exhibits an extended conformation, showing a large radius of gyration (R_G = 19.1 Å, Figure 4A, left conformation), which is a good measure of the ensemble average of polymer size.[36] In sharp contrast, the polymer is substantially collapsed at low pH, with a reduced R_G of only 11.6 Å (Figure 4A, right conformation). This nanoscale change in conformation arises from increased intramolecular hydrogen bonds between the pendant groups on a single polymer backbone (and also between chains) under acidic conditions (indicated by red lines in Figure 4A, right conformation). Molecular dynamics (MD) simulations of the aforementioned model polymer chains further support the MC results: at pH 7.4 and 300 K, the deprotonated poly(AAc-*r*-AAm) exhibits a calculated R_G of 20.5 ± 0.8 Å (see additional discussion below), which is reduced to 11.8 ± 0.3 Å at pH 5.0.

When many of these polymer chains are cross-linked together across the whole liposomal membrane, their acid-triggered conformational collapse cooperatively creates a dense network of pressured points that "squeezes" the liposome (Figure 4B,C), greatly destabilizing the lipid bilayer membrane and leading to a significant enhancement of drug release from the liposomal core.[37] Without the cross-linking between chains, acid-triggered conformational change of the individual polymer chains can only result in relatively small "point defects" on the membrane rather than a concerted destabilization of liposome *via* the "squeezing" action of the densified polymer cage.

Testing the Model *via* Temperature Changes. Poly(AAc-*r*-AAm) is well-known to exhibit thermosensitive swelling/shrinking behavior, a property that arises from its lower critical solution temperature (LCST), which ranges between 30 and 40 °C.[31,38] At LCST, this copolymer undergoes a temperature-dependent random-coil-to-globule phase transition induced by the segregation of polymer chains from the surrounding water molecules. As a result, the increased intermolecular hydrophobic interactions between the polymer chains above the LCST eventually lead to the globular aggregation of polymer networks out of the aqueous solution. We hypothesize that such thermally driven swelling/shrinking behavior may also occur as a function of temperature in our model poly(AAc-*r*-AAm) chain and can be observed computationally.

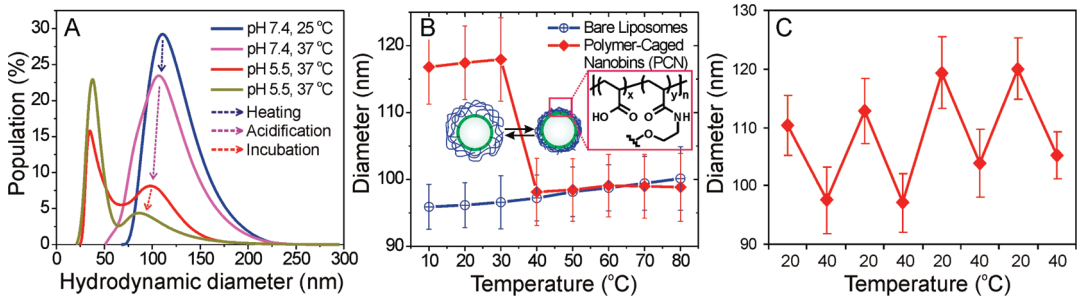

Figure 6. (A) Hydrodynamic diameter (D_H) profiles of PCN(emp) as measured by dynamic light scattering under various stimulus conditions. (B) Temperature-dependent change in the mean hydrodynamic diameter of PCN(emp) and BL(emp). Also shown for comparison is the temperature-dependent mean diameter of BL(emp). Overlaid on top of the plots is a schematic drawing of the reversible swelling/shrinking property of the cross-linked polymer cage in PCN(emp). (C) Experimentally determined D_H profile showing the reversible size changes of PCN(emp) in the 20−40 °C range (PCN(emp) solution was incubated for 30 min at each temperature for equilibration prior to D_H measurements).

Molecular dynamics simulations were thus carried out with the aforementioned poly(AAc-*r*-AAm) model polymer as a molecular analogue for our polymer cage under neutral aqueous conditions and at either 290 or 330 K. As expected, the R_G population of the polymer chain varies inversely as a function of temperature: the average R_G at 290 K was found to be 22.4 ± 1.1 Å (Figure 5A), decreasing to 20.5 ± 0.9 Å at 330 K (Figure 5B). Although this temperature-dependent change in R_G was relatively small (ΔR_G = 1.9 Å over a 40 K range) compared to the aforementioned pH-induced size change (ΔR_G = 7.5 Å over a 2.4 pH unit change), these results clearly support the temperature-sensitive shrinking property of the cross-linked polymer cage in our PCN platform.

Experimental Tests of Predicted PCN Size Changes in Response to Thermal and pH Stimuli. To test the aforementioned predicted pH- and temperature-induced size changes of the PCN platform, we compared the hydrodynamic diameter of a model empty liposome system, BL(emp), against that of an empty PCN, PCN(emp), under various stimulus conditions using dynamic light scattering. At pH 7.4 and 25 °C, the mean D_H of this PCN(emp) was 121 ± 25 nm. This value decreased to 108 ± 27 nm when the temperature was increased to 37 °C (blue dotted arrow in Figure 6A), as predicted by our MD simulations. Consistent with the analogy of a phase transition, a separate temperature-variation experiment showed the mean D_H of our PCN(emp) model system being constant (118 ± 11 nm) in the 10−30 °C range, undergoing ~20% decrease (D_H = 99 ± 9 nm) as the temperature is increased above 40 °C, and then remaining constant at the smaller value up to 80 °C (Figure 6B). In stark contrast, the parent BL(emp) system exhibits only an insignificant diameter expansion that is typically observed with temperature increase over the same temperature range. Given the highly stable nature of the lipid membranes used in our model systems (containing 40 mol % of cholesterol, which eliminates the melting transition of the lipid bilayer[39]), the decrease of the PCN(emp)'s D_H above 40 °C can be attributed solely to the conformational change of its outer polymer cage. As predicted from our MD simulations, the relatively small change in R_G upon temperature variation (ΔR_G = 1.9 Å, ~10%) is not enough of a driving force to result in PCN membrane rupture. Not surprisingly, this thermally induced conformational change in the polymer cage is completely reversible without hampering the membrane integrity of PCN (Figure 6C). The Ni^{II}-to-lipid and As^{III}-to-lipid ratios in PCN(Ni,As) samples that were incubated at 40 °C for 2 h are the same as those for PCN(Ni,As) samples that were incubated at 25 °C (Figure S6 in the SI), further confirming that there was minimum drug leakage from PCN(Ni,As) when its size becomes smaller at the higher temperature.

Given that the polymer cage in our model PCN(emp) system resembles a cross-linked network of poly(AAc-*r*-AAm), a large change in D_H should be observed when the solution becomes acidic.[40] At 37 °C, the D_H of PCN(emp) further decreased to 69 ± 39 nm upon acidification to pH 5.5 (from pH 7.4, purple arrow in Figure 6A). Longer incubation at pH 5.5 and 37 °C further decreased the D_H of PCN(emp) to 49 ± 26 nm (red arrow in Figure 6A). Consistent with our modeling results, these pH-induced changes in PCN size are much larger than the thermally induced changes and can significantly affect the stability of the caged liposome, eventually leading to its rupture and observed enhancements in drug-release. Indeed, as shown in the first part of this paper, the pH-sensitive polymer cage of PCN is the main contributor to the concurrent release of both Ni^{II} and As^{III} agents from a liposomal core, in stark contrast to the sole release of As^{III} from BL(Ni,As).

CONCLUSION

In conclusion, the versatile tunable release property of the PCN platform can be attributed to the pH- and temperature-responsive conformation change of a cross-linked polymer network on the nanoscale: this is corroborated by computational modeling studies and verified in PCN model systems. As demonstrated here, the resulting concurrent release of multiple chemotherapeutic agents can lead to improved therapeutic index,

where Ni^{II} ions can cooperatively enhance the pro-apoptotic activity of arsenic trioxide while reducing its detrimental side effects. The ability to acid-trigger the release of a combination of drugs co-encapsulated in a single nanoparticle *via* chemomechanical perturbation of a modified liposomal membrane is a key feature that enhances PCN as a drug delivery platform, particular for disease sites that have low pH's. The delivery of anticancer drugs to hypoxic, acidic tumor tissues using the PCN platform provides several advantageous features relative to bare liposome, and we anticipate that they will be effective for delivering a variety of drugs[41] to cancer cells that take up nanoparticles *via* an endocytotic pathway and process them through acidic lysosomes.

MATERIALS AND METHODS

Materials. Unless otherwise noted, all reagents and materials were purchased from commercial sources and used as received. 1,2-Dipalmitoyl-*sn*-glycero-3-phosphocholine (DPPC) and 1,2-dioleoyl-*sn*-glycero-3-[phospho-*rac*-(1-glycerol)] (sodium salt) (DOPG) were purchased from Avanti Polar Lipids (Alabaster, AL). ICP calibration standard solutions of phosphorus (1000 μg/mL P), 1-(3-dimethylaminopropyl)-3-ethylcarbodiimide methiodide (EDC·MeI), 2,2′-(ethylenedioxy)bis(ethyleneamine), and all other reagents were purchased from Aldrich Chemical Co. (Milwaukee, WI). Cholesterol-terminated poly(acrylic acid) was prepared using a literature procedure.[20] Ultrapure deionized (DI) water was obtained from a Millipore system (18.2 MΩ cm resistivity).

Instrumentation. Fourier-transformed nuclear magnetic resonance (NMR) spectroscopy was performed on a Varian INOVA-500 MHz spectrometer (^{1}H = 499.6 MHz). Chemical shifts of ^{1}H NMR spectra are reported in ppm against residual solvent resonance as the internal standard ($CHCl_3$ = 7.27 ppm, CHD_2COCD_3 = 2.05 ppm, CHD_2OD = 3.31 ppm, D_2O = 4.8 ppm). UV−vis absorption spectra were obtained on a CARY 300 Bio UV−vis spectrophotometer.

Electrospray-ionization mass spectrometric (ESIMS) data were obtained on a Micromass Quattro II triple quadrupole mass spectrometer. Phosphorus, arsenic, and nickel concentrations of the synthesized liposome and PCN materials and of the Sephadex-eluted liposome fractions in benchtop-release experiments were determined using a Varian Vista MPX simultaneous inductively coupled plasma optical emission (ICP-OES) spectrometer.

Polymer molecular weight of the cholesterol-terminated poly(*tert*-butyl acrylate) was measured relative to polystyrene standards on a Waters gel-permeation chromatograph equipped with Breeze software, a 717 autosampler, a Shodex KF-G guard column, KF-803 L and KF-806 L columns in series, a Waters 2440 UV detector, and a 410 RI detector. HPLC-grade THF was used as an eluent at a flow rate of 1.0 mL/min, and the instrument was calibrated using polystyrene standards (Aldrich, 15 standards, 760−1 800 000 Da).

Dynamic light scattering and zeta potential measurements were performed on a Zetasizer Nano ZS (Marvern Instruments, Malvern, UK) with a He−Ne laser (633 nm). The noninvasive backscatter method (detection at 173° scattering angle) was used. Correlation data were fitted, using the method of cumulants, to the logarithm of the correlation function, yielding the diffusion coefficient, D. The hydrodynamic diameters of the BLs and PCNs were calculated using D and the Stokes−Einstein equation ($D_H = k_BT/3\pi\eta D$, where k_B is the Boltzmann constant, T is the absolute temperature, and η is the solvent viscosity (η = 0.8872 cP for water)). The polydispersity index of liposomes—represented as $2c/b^2$, where b and c are first- and second-order coefficients, respectively, in a polynomial of a semilog correlation function—was calculated by the cumulants analysis. Size distribution of vesicles was obtained by nonnegative least-squares analysis. Unless noted otherwise, all samples were dispersed in 10 mM HEPES solution (pH 7.4, 150 mM NaCl) for the measurements. The data reported represent an average of 10 measurements with five scans each.

For *in vitro* assays, drug solutions were transferred with a Beckman Coulter Biomek FX 96 multichannel robotic liquid handler (Beckman Coulter, Brea, CA), and MTS cell proliferation assays were monitored by Analyst GT Multimode Reader (Molecular Devices, Sunnyvale, CA) at NU High Throughput Analysis Laboratory (NU-HTA).

Preparation of [Ni^{II}, As^{III}]-Loaded Polymer-Caged Nanobins, PCN(Ni, As). [Ni^{II}, As^{III}]-loaded bare liposome was prepared using a modified literature procedure.[6] DPPC (108.29 μmol), DOPG (6.91 μmol), and cholesterol (76.8 μmol, 40 mol % of the total membrane components; this number is chosen to eliminate the thermal instability of the liposomes that is attributable to the intrinsic phase-transition temperature of the lipid) were added to a 20 mL cylindrical glass vial, followed by chloroform (5 mL) to make a colorless solution. After vortexing (~1 min), the solvent was removed by passing a stream of nitrogen over the solution while the vial was warmed in a 50 °C water bath. The resulting dry film was further dried under vacuum on a Schlenk line (<30 mTorr) overnight. Next, the dry lipid films were hydrated in 300 mM aqueous [$Ni(CH_3COO)_2$] solution (5 mL) followed by vigorous vortexing (3−5 min on a Vortex Mixer, American Scientific Products) to form a dispersion of multilamellar vesicles. After this dispersion was subjected to 10 freeze−thaw cycles, it was extruded 10 times through two stacked polycarbonate extrusion membranes (100 nm pore size) that are maintained at 50 °C in a LIPEX extruder (Northern Lipids Inc., Burnaby, BC, Canada). The excess [$Ni(CH_3COO)_2$] outside of the liposome was removed by Sephadex G-50 (50 mL) gel-filtration chromatography pre-equilibrated with 150 mM NaCl solution. Aqueous arsenic trioxide (ATO, 0.5 equiv of the total lipid content) solution was added to the collected liposome solution (~5 mL of a solution with ~4 mM lipid concentration) and incubated at 50 °C for 3 h. The excess ATO outside of the liposome was then removed by Sephadex G-50 (50 mL) gel-filtration chromatography pre-equilibrated with 20 mM HEPES buffers (pH 7.4, 150 mM NaCl). The loading of the Ni^{II} and As^{III} was determined by ICP-OES. Mean hydrodynamic diameter of 97 ± 8 nm was determined by DLS measurements.

The [Ni^{II}, As^{III}]-loaded bare liposomes, BL(Ni,As), were next subjected to the PCN fabrication process as reported previously.[20] For this process, 10 mol % of the cholesterol-terminated poly(acrylic acid) (Chol-PAA, $\bar{M}_n \approx$ 3700 Da) was chosen to maximize the amount of the modifier while preventing local phase-segregation of all the cholesterol in the membrane. Next, 50% of acrylate repeating units in Chol-PAA chains was cross-linked with diamine cross-linker. Mean D_H of 125 ± 14 nm and −14.2 mV of zeta potential were determined by DLS measurements. To measure the stimuli-sensitive diameter change of PCN particles, the same preparation method described above was carried out with an empty bare liposome template.

[Ni^{II}, As^{III}]-Release Assay from PCN(Ni,As). PCN(Ni,As) solutions (1 mM, 2 mL) were added into a semipermeable dialysis tube (molecular weight cutoff 10 kDa) and dialyzed against either 20 mM acetate buffer (pH 4.0, 150 mM NaCl) or 20 mM HEPES buffer (pH 7.4, 150 mM NaCl) at 37 °C with stirring. An aliquot of the PCN(Ni,As) was collected at a predetermined time, and the Ni^{II}, As^{III}, and lipid (P) contents were measured by ICP-OES. The extent of drug release was observed by comparing time-dependent change of Ni^{II}/P and As^{III}/P molar ratios to the initial values.

Cell Culture. *a. Media and Cell Culture Reagents.* Eagle's minimum essential medium (EMEM) was purchased from ATCC

(Manassas, VA), and trypsin solution (0.25%, containing EDTA) was purchased from Invitrogen (San Diego, CA). Fetal bovine serum (FBS), penicillin–streptomycin, and phosphate-buffered saline (PBS, 1× without calcium and magnesium) solutions were purchased from Mediatech (Manassas, VA).

b. Cell Lines and Conditions. HeLa human cervical cancer cells (CCL-2) were purchased from American Type Culture Collection (ATCC, Manassas, VA). HeLa cells were continuously cultured in EMEM supplemented with 10 vol % heat-inactivated FBS and 0.5 vol % penicillin–streptomycin solution at 37 °C in a humidified atmosphere containing 5% CO_2.

Cytotoxicity Assays. The cells (20 000) were seeded into 96-well plates (100 μL/well). The plates were then incubated under the cell culture conditions, and the cells were allowed to grow to confluence for 24 h. The media in the wells was replaced with the preprepared growth media containing the appropriate drug formulation (100 μL of solution at the appropriate As^{III} concentrations). The drug-treated cells were incubated for either 48, 72, or 96 h under the cell culture conditions, after which the cells were washed with PBS buffer (2 × 150 μL). The cell viabilities were then measured by the MTS cell proliferation assay, and the relative cell survival percentages compared to the drug-free control were plotted against the drug concentration in logarithmic scale. The data reported represent an average of three measurements from different batches. The dose–effect profiles were obtained by sigmoidal logistic fitting using Origin 6.1 (OriginLab, Northampton, MA), and the half-maximal inhibitory concentration (IC_{50}) values were determined on the basis of the fitted data.

Apoptosis Assay. Flow cytometry with a Guava Nexin Apoptosis Assay kit (annexin V-PE/7-AAD, Millipore) was used to determine apoptotic cell populations. HeLa cells (100 000) were seeded into a 24-well tissue culture plate and incubated for 24 h under standard growth conditions. Cell-growth media was then replaced with fresh media including PCN(Ni,As), BL(Ni,As), or ATO ($[As^{III}]$ = 10 μM for each drug formulation). The drug-treated cells were incubated for 48 h under the cell culture conditions, after which the cells were washed with PBS buffer. The cells were then detached by harvesting with 0.25% trypsin-EDTA solution and subsequently stained by the Guava Nexin reagent. Then, the apoptotic cell population was measured using a Guava EasyCyte Mini flow cytometer. The data reported represent an average of three measurements from different batches.

Molecular Modeling. *a. Monte Carlo Simulation.* The AMBER* parameters implemented in Macromodel 6.0[42] were used for the Monte Carlo conformational search[35] and molecular mechanics calculations of the polymer shown in Figure 4 to obtain the minimum energy structures. The GB/SA method[43] is used for simulating water solvent, and the number of structures tried in the conformational search was 1000. Energy minimization based on the conjugate gradient algorithm was then performed on every sampled structure to a gradient norm of less than 0.01 $kJ \cdot mol^{-1}$ $Å^{-1}$.

b. Molecular Dynamics Simulations. Molecular dynamics simulations of the polymer shown in Figure 4 at virtual pH 7.4 and either 290 or 330 K—as well as at virtual pH 5.0 or 7.4 at 300 K—were performed using the Monte Carlo/Stochastic Dynamics (MC/SD)[44] method implemented in Macromodel 6.0. A production simulation was performed for 1 ns after 10 ps equilibration with a 1 fs time step. The GB/SA method was again used for simulating water solvent, and atomic coordinates were saved every 1 ps for the calculation of the radius of gyration.

Acknowledgment. This work was financially supported by the NIH (NCI Center of Cancer Nanotechnology Excellence Grants U54CA119341 Project 4 and U54CA151880 Core, Cancer Nanotechnology Platform Partnerships Grant U01CA151461, and Core Grant P30CA060553 to the Robert H. Lurie Comprehensive Cancer Center of Northwestern University). Instruments in the Northwestern IMSERC and QBIC facilities were purchased with grants from NSF-NSEC, NSF-MRSEC, Keck Foundation, the state of Illinois, NASA, and Northwestern University. G.C.S. and O.S.L. acknowledge NSF grant CHE-0843823. We acknowledge the use of instruments in the NU-HTA facilities. We thank Dr. Haimei Chen and Dr. Richard W. Ahn for their helpful discussions.

Supporting Information Available: Schematic illustration of the IGM loading of As^{III}, DLS data of PCN(Ni,As), drug release profiles of PCN(Ni,As) at neutral conditions, apoptosis analyses of As^{III}-drug formulations with HeLa cells, and temperature-dependent drug leakage of PCN(Ni,As). This material is available free of charge *via* the Internet at http://pubs.acs.org.

REFERENCES AND NOTES

1. Torchilin, V. P. Recent Advances with Liposomes as Pharmaceutical Carriers. *Nat. Rev. Drug Discovery* **2005,** *4*, 145–160.
2. Drummond, D. C.; Meyer, O.; Hong, K.; Kirpotin, D. B.; Papahadjopoulos, D. Optimizing Liposomes for Delivery of Chemotherapeutic Agents to Solid Tumors. *Pharmacol. Rev.* **1999,** *51*, 691–744.
3. Barenholz, Y.; Amselem, S.; Goren, D.; Cohen, R.; Gelvan, D.; Samuni, A.; Golden, E. B.; Gabizon, A. Stability of Liposomal Doxorubicin Formulations: Problems and Prospects. *Med. Res. Rev.* **1993,** *13*, 449–491.
4. Allen, T. M. Liposomal Drug Formulations: Rationale for Development and What We Can Expect for the Future. *Drugs* **1998,** *56*, 747–756.
5. Waterhouse, D. N.; Tardi, P. G.; Mayer, L. D.; Bally, M. B. A Comparison of Liposomal Formulations of Doxorubicin with Drug Administered in Free Form: Changing Toxicity Profiles. *Drug Safety* **2001,** *24*, 903–920.
6. Chen, H.; MacDonald, R. C.; Li, S.; Krett, N. L.; Rosen, S. T.; O'Halloran, T. V. Lipid Encapsulation of Arsenic Trioxide Attenuates Cytotoxicity and Allows for Controlled Anticancer Drug Release. *J. Am. Chem. Soc.* **2006,** *128*, 13348–13349.
7. Chen, H.; Pazicni, S.; Krett, N. L.; Ahn, R. W.; Penner-Hahn, J. E.; Rosen, S. T.; O'Halloran, T. V. Coencapsulation of Arsenic- and Platinum-Based Drugs for Targeted Cancer Treatment. *Angew. Chem., Int. Ed.* **2009,** *48*, 9295–9299.
8. Miller, W. H.; Schipper, H. M.; Lee, J. S.; Singer, J.; Waxman, S. Mechanisms of Action of Arsenic Trioxide. *Cancer Res.* **2002,** *62*, 3893–3903.
9. Platanias, L. C. Biological Responses to Arsenic Compounds. *J. Biol. Chem.* **2009,** *284*, 18583–18587.
10. Zhu, J.; Chen, Z.; Lallemand-Breitenbach, V.; de The, H. How Acute Promyelocytic Leukaemia Revived Arsenic. *Nat. Rev. Cancer* **2002,** *2*, 705–714.
11. Uslu, R.; Sanli, U. A.; Sezgin, C.; Karabulut, B.; Terzioglu, E.; Omay, S. B.; Goker, E. Arsenic Trioxide-Mediated Cytotoxicity and Apoptosis in Prostate and Ovarian Carcinoma Cell Lines. *Clin. Cancer Res.* **2000,** *6*, 4957–4964.
12. Ahn, R. W.; Chen, F.; Chen, H.; Stern, S. T.; Clogston, J. D.; Patri, A. K.; Raja, M. R.; Swindell, E. P.; Parimi, V.; Cryns, V. L.; O'Halloran, T. V. A Novel Nanoparticulate Formulation of Arsenic Trioxide with Enhanced Therapeutic Efficacy in a Murine Model of Breast Cancer. *Clin. Cancer Res.* **2010,** *16*, 3607–3617.
13. Chen, H.; Ahn, R.; Van den Bossche, J.; Thompson, D. H.; O'Halloran, T. V. Folate-Mediated Intracellular Drug Delivery Increases the Anticancer Efficacy of Nanoparticulate Formulation of Arsenic Trioxide. *Mol. Cancer Ther.* **2009,** *8*, 1955–1963.
14. Salnikow, K.; Donald, S. P.; Bruick, R. K.; Zhitkovich, A.; Phang, J. M.; Kasprzak, K. S. Depletion of Intracellular Ascorbate by the Carcinogenic Metals Nickel and Cobalt Results in the Induction of Hypoxic Stress. *J. Biol. Chem.* **2004,** *279*, 40337–40344.
15. Lee, S.-M.; Chen, H.; O'Halloran, T. V.; Nguyen, S. T. 'Clickable' Polymer-Caged Nanobins as a Modular Drug Delivery Platform. *J. Am. Chem. Soc.* **2009,** *131*, 9311–9320.
16. Tannock, I. F.; Rotin, D. Acid pH in Tumors and Its Potential for Therapeutic Exploitation. *Cancer Res.* **1989,** *49*, 4373–4384.
17. Casey, J. R.; Grinstein, S.; Orlowski, J. Sensors and Regulators of Intracellular pH. *Nat. Rev. Mol. Cell Biol.* **2010,** *11*, 50–61.

18. Sadiq, M. *Arsenic Chemistry in Soils: An Overview of Thermodynamic Predictions and Field Observations*; Springer: The Netherlands, 1997; Vol. 93, pp 117−136.
19. Huang, H.; Kowalewski, T.; Remsen, E. E.; Gertzmann, R.; Wooley, K. L. Hydrogel-Coated Glassy Nanospheres: A Novel Method for the Synthesis of Shell Cross-Linked Knedels. *J. Am. Chem. Soc.* **1997,** *119*, 11653–11659.
20. Lee, S.-M.; Chen, H.; Dettmer, C. M.; O'Halloran, T. V.; Nguyen, S. T. Polymer-Caged Liposomes: A pH-Responsive Delivery System with High Stability. *J. Am. Chem. Soc.* **2007,** *129*, 15096–15097.
21. Gulati, M.; Grover, M.; Singh, S.; Singh, M. Lipophilic Drug Derivatives in Liposomes. *Int. J. Pharm.* **1998,** *165*, 129–168.
22. VanEngeland, M.; Nieland, L. J. W.; Ramaekers, F. C. S.; Schutte, B.; Reutelingsperger, C. P. M. Annexin V-Affinity Assay: A Review on an Apoptosis Detection System Based on Phosphatidylserine Exposure. *Cytometry* **1998,** *31*, 1–9.
23. Savic, R.; Luo, L.; Eisenberg, A.; Maysinger, D. Micellar Nanocontainers Distribute to Defined Cytoplasmic Organelles. *Science* **2003,** *300*, 615–618.
24. Barltrop, J. A.; Owen, T. C.; Cory, A. H.; Cory, J. G. 5-(3-Carboxymethoxyphenyl)-2-(4,5-Dimethylthiazolyl)-3-(4-Sulfophenyl)Tetrazolium, Inner Salt (MTS) and Related Analogs of 3-(4,5-Dimethylthiazolyl)-2,5-Diphenyltetrazolium Bromide (MTT) Reducing to Purple Water-Soluble Formazans as Cell-Viability Indicators. *Bioorg. Med. Chem. Lett.* **1991,** *1*, 611–614.
25. Gerasimov, O. V.; Boomer, J. A.; Qualls, M. M.; Thompson, D. H. Cytosolic Drug Delivery Using pH- and Light-Sensitive Liposomes. *Adv. Drug Delivery Rev.* **1999,** *38*, 317–338.
26. Liu, S. X.; Athar, M.; Lippai, I.; Waldren, C.; Hei, T. K. Induction of Oxyradicals by Arsenic: Implication for Mechanism of Genotoxicity. *Proc. Natl. Acad. Sci. U. S. A.* **2001,** *98*, 1643–1648.
27. Smith, D.; Clark, S. H.; Bertin, P. A.; Mirkin, B. L.; Nguyen, S. T. Synthesis and in Vitro Activity of ROMP-Based Polymer Nanoparticles. *J. Mater. Chem.* **2009,** *19*, 2159–2165.
28. Lee, S.-M.; Ahn, R. W.; Chen, F.; Fought, A. J.; O'Halloran, T. V.; Cryns, V. L.; Nguyen, S. T. Biological Evaluation of pH-Responsive Polymer-Caged Nanobins for Breast Cancer Therapy. *ACS Nano* **2010,** *4*, 4971–4978.
29. Lee, C. C.; Gillies, E. R.; Fox, M. E.; Guillaudeu, S. J.; Fréchet, J. M. J.; Dy, E. E.; Szoka, F. C. A Single Dose of Doxorubicin-Functionalized Bow-Tie Dendrimer Cures Mice Bearing C-26 Colon Carcinomas. *Proc. Natl. Acad. Sci. U. S. A.* **2006,** *103*, 16649–16654.
30. Maeda, H.; Wu, J.; Sawa, T.; Matsumura, Y.; Hori, K. Tumor Vascular Permeability and the EPR Effect in Macromolecular Therapeutics: A Review. *J. Controlled Release* **2000,** *65*, 271–284.
31. Chen, G.; Hoffman, A. S. Graft Copolymers That Exhibit Temperature-Induced Phase Transitions over a Wide Range of pH. *Nature* **1995,** *373*, 49–52.
32. Tanaka, T.; Fillmore, D.; Sun, S.-T.; Nishio, I.; Swislow, G.; Shah, A. Phase Transitions in Ionic Gels. *Phys. Rev. Lett.* **1980,** *45*, 1636.
33. Huggins, M. L. Solutions of Long Chain Compounds. *J. Chem. Phys.* **1941,** *9*, 440–440.
34. Flory, P. J. Thermodynamics of High Polymer Solutions. *J. Chem. Phys.* **1942,** *10*, 51–61.
35. Chang, G.; Guida, W. C.; Still, W. C. An Internal-Coordinate Monte Carlo Method for Searching Conformational Space. *J. Am. Chem. Soc.* **1989,** *111*, 4379–4386.
36. Dautenhahn, J.; Hall, C. K. Monte Carlo Simulation of Off-Lattice Polymer Chains: Effective Pair Potentials in Dilute Solution. *Macromolecules* **1994,** *27*, 5399–5412.
37. Leroux, J.-C.; Roux, E.; Le Garrec, D.; Hong, K.; Drummond, D. C. N-Isopropylacrylamide Copolymers for the Preparation of pH-Sensitive Liposomes and Polymeric Micelles. *J. Controlled Release* **2001,** *72*, 71–84.
38. Nayak, S.; Lyon, L. A. Soft Nanotechnology with Soft Nanoparticles. *Angew. Chem., Int. Ed.* **2005,** *44*, 7686–7708.
39. Hinz, H.-J.; Sturtevant, J. M. Calorimetric Investigation of the Influence of Cholesterol on the Transition Properties of Bilayers Formed from Synthetic L-α-Lecithins in Aqueous Suspension. *J. Biol. Chem.* **1972,** *247*, 3697–3700.
40. Turner, J. L.; Wooley, K. L. Nanoscale Cage-Like Structures Derived from Polyisoprene-Containing Shell Cross-Linked Nanoparticle Templates. *Nano Lett.* **2004,** *4*, 683–688.
41. Lee, S.-M.; O'Halloran, T. V.; Nguyen, S. T. Polymer-Caged Nanobins for Synergistic Cisplatin-Doxorubicin Combination Chemotherapy. *J. Am. Chem. Soc.* **2010,** *132*, 17130–17138.
42. Mohamadi, F.; Richards, N. G. J.; Guida, W. C.; Liskamp, R.; Lipton, M.; Caufield, C.; Chang, G.; Hendrickson, T.; Still, W. C. Macromodel—an Integrated Software System for Modeling Organic and Bioorganic Molecules Using Molecular Mechanics. *J. Comput. Chem.* **1990,** *11*, 440–467.
43. Qiu, D.; Shenkin, P. S.; Hollinger, F. P.; Still, W. C. The GB/SA Continuum Model for Solvation. A Fast Analytical Method for the Calculation of Approximate Born Radii. *J. Phys. Chem. A* **1997,** *101*, 3005–3014.
44. Guarnieri, F.; Still, W. C. A Rapidly Convergent Simulation Method: Mixed Monte Carlo/Stochastic Dynamics. *J. Comput. Chem.* **1994,** *15*, 1302–1310.